RESEARCH ARTICLE

An Integrated Assessment Model for Helping the United States Sea Scallop (*Placopecten magellanicus*) Fishery Plan Ahead for Ocean Acidification and Warming

Sarah R. Cooley[1,2☯]*, **Jennie E. Rheuban[2☯]**, **Deborah R. Hart[3☯]**, **Victoria Luu[4☯]**, **David M. Glover[2☯]**, **Jonathan A. Hare[5☯]**, **Scott C. Doney[2☯]**

1 Ocean Conservancy, Washington, DC, United States of America, **2** Department of Marine Chemistry and Geochemistry, Woods Hole Oceanographic Institution, Woods Hole, Massachusetts, United States of America, **3** NOAA NMFS NEFSC Woods Hole Laboratory, Woods Hole, Massachusetts, United States of America, **4** Department of Earth and Environmental Sciences, Boston College, Chestnut Hill, Massachusetts, United States of America, **5** NOAA NMFS NEFSC Narragansett Laboratory, Narragansett, Rhode Island, United States of America

☯ These authors contributed equally to this work.
* scooley@oceanconservancy.org

Abstract

Ocean acidification, the progressive change in ocean chemistry caused by uptake of atmospheric CO_2, is likely to affect some marine resources negatively, including shellfish. The Atlantic sea scallop (*Placopecten magellanicus*) supports one of the most economically important single-species commercial fisheries in the United States. Careful management appears to be the most powerful short-term factor affecting scallop populations, but in the coming decades scallops will be increasingly influenced by global environmental changes such as ocean warming and ocean acidification. In this paper, we describe an integrated assessment model (IAM) that numerically simulates oceanographic, population dynamic, and socioeconomic relationships for the U.S. commercial sea scallop fishery. Our primary goal is to enrich resource management deliberations by offering both short- and long-term insight into the system and generating detailed policy-relevant information about the relative effects of ocean acidification, temperature rise, fishing pressure, and socioeconomic factors on the fishery using a simplified model system. Starting with relationships and data used now for sea scallop fishery management, the model adds socioeconomic decision making based on static economic theory and includes ocean biogeochemical change resulting from CO_2 emissions. The model skillfully reproduces scallop population dynamics, market dynamics, and seawater carbonate chemistry since 2000. It indicates sea scallop harvests could decline substantially by 2050 under RCP 8.5 CO_2 emissions and current harvest rules, assuming that ocean acidification affects *P. magellanicus* by decreasing recruitment and slowing growth, and that ocean warming increases growth. Future work will explore different economic and management scenarios and test how potential impacts of ocean acidification on other scallop

biological parameters may influence the social-ecological system. Future empirical work on the effect of ocean acidification on sea scallops is also needed.
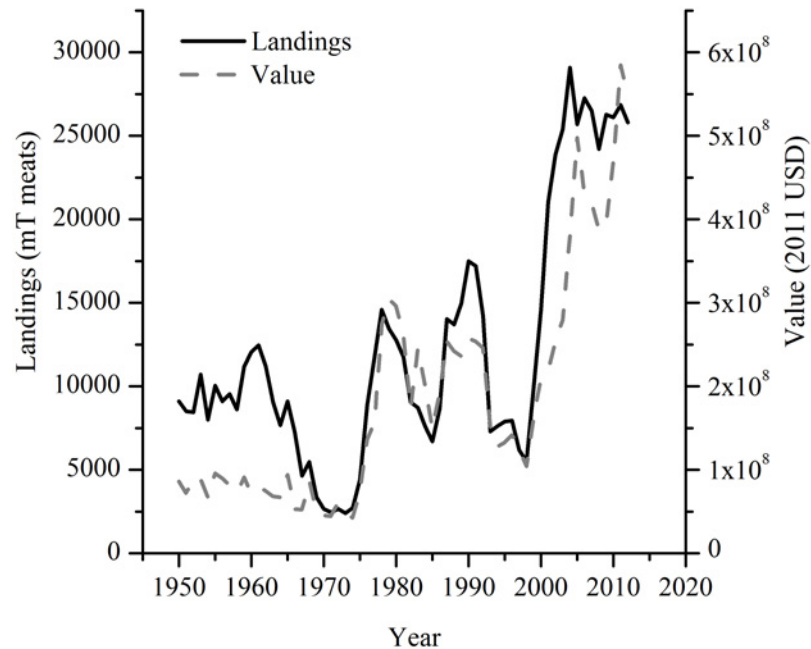
Introduction

Fisheries science has long incorporated the effects of fishing, a human perturbation, into marine harvest advice as well as short and long-term forecasts (e.g., [1]). However, including the effects of other anthropogenically driven global changes, like warming and changing water chemistry, is relatively new [2–7]. Additionally, socioeconomic factors influence marine policy and management significantly, yet they have been traditionally given less attention and separate treatment [8]. One reason for this relatively slow incorporation of global change into fisheries advice is that it remains challenging to distinguish the effects of climate, particularly temperature rise, from those of fishing and natural environmental or biological stochasticity in many contexts [9], and references therein). Another reason is the different timescales of concern: fisheries plans are developed every few years, whereas effects of global change occur progressively over decades. Planning for present and future fishery harvests against a background of global change, though, requires understanding how both short- and long-term processes associated with environmental and social factors affect the fishery through direct and indirect routes [10]. Integrated assessment models (IAMs) that numerically simulate oceanographic, population dynamic, and socioeconomic relationships provide one way to bring together these disciplines and provide both short- and long-term perspectives on how different components of the social-ecological system affect each other. In their simplest forms, IAMs can be developed for single-species fisheries that are subject to a limited set of major environmental and human influences and whose socioeconomic importance is relatively easy to quantify monetarily.

Atlantic sea scallop

Atlantic sea scallops (*Placopecten magellanicus*) support one of the most economically important single-species fisheries in the United States. They are found along the eastern North American continental shelf from Virginia to the Gulf of Maine and north into Canada, but primary harvest areas in the U.S. are located in the Mid-Atlantic Bight and Georges Bank, between 35 and 100m depth [11]. A small Gulf of Maine population is in nearshore, shallow, state waters and comprises only a few percent of the annual harvest each year [12]. Most sea scallops are typically found in waters that remain below 17°C and above 0°C, although they can tolerate temperatures as high as 20°C [11]. Larvae remain planktonic in the upper water column for the first 4–7 weeks of life before settling to the bottom. Scallops become sexually mature at around age 2, reach a commercially harvestable size at about age 4 (90 mm), and can reach ages of at least 18–20 years, with a maximal shell height ranging from 125–180 mm [13,14]. Populations living in the Mid-Atlantic and Georges Bank regions have slightly different growth parameters; the Mid-Atlantic population reaches a lower average maximum size, but at a slightly faster rate, compared to that farther north [14].

The sea scallop fishery, which grossed $559 million in dockside revenue in 2012 [15] (Fig 1), is intensively managed with an area rotational management scheme that includes limited permits and restrictions on days at sea, gear size, and crew size [16]. Regular population surveys inform the spatial area management simulator (SAMS) and a catch-at-size-analysis (CASA) model [12,17], which provide information used in the determination of allowable catch limits. Although careful management appears to be the most powerful short-term

Fig 1. US sea scallop harvests through time (NMFS commercial harvest data accessed January 28, 2014). Values are adjusted to 2011 US dollars.

factor that affects scallop populations [16], scallops will be increasingly influenced by long-term global environmental change in the coming decades as bottom temperatures rise [18] and ocean acidification advances.

Ocean acidification

Ocean acidification refers to a series of chemical changes caused by the uptake of CO_2 into seawater: elevated aqueous CO_2 and total inorganic carbon, and reduced pH, carbonate ion, and calcium carbonate mineral saturation states [19]. Fossil fuel combustion and deforestation have caused global mean atmospheric CO_2 levels to grow by 40% from about 280 ppm in the preindustrial era to 396 ppm by 2013 (www.esrl.noaa.gov/gmd/ccgg/trends/), causing a net global air-to-sea flux of excess CO_2 that dissolves about 25% of total anthropogenic carbon emissions in seawater [20]. Consequently, sea-surface pH is estimated to have dropped by 0.1 pH units since the preindustrial era, a 26% increase in acidity over the past 150 years, mostly in the past several decades. Future projections suggest declines of an additional 0.2–0.3 pH units over this century [21]. At the same time, global sea surface temperatures have increased by 0.8°C with substantial regional variability [22].

On the continental shelf in the Mid-Atlantic Bight and Georges Bank, mean summertime sea surface saturation state of aragonite (Ω_{ar}), a more soluble mineral form of calcium carbonate and one commonly found in larval bivalve shells, declines towards the north, beginning at around Ω_{ar} = 3 east of North Carolina, decreasing to 2.5 southeast of Massachusetts, and to 1.9 east of New Hampshire [23,24]. In winter, the south to north gradient still exists, but overall levels are lower ranging from Ω_{ar} = 2.2 east of North Carolina and 1.5 east of New Hampshire [23]. The response of *P. magellanicus* to calcium carbonate saturation state has not been determined experimentally, but other observed species-specific responses to ocean acidification among mollusks [e.g., Eastern oyster, (*Crassostrea virginica*, *Osteridae*); hard clam (*Mercenaria mercenaria*); Atlantic bay scallop (*Argopecten irradians*, *Pectinidae*)] have been mostly neutral

or negative and affect growth, survival, and development (e.g., [25–29]). The king scallop, (*P. maximus*), which is taxonomically close to *P. magellanicus* and has a very similar life history, also shows reduced growth and energy budgets under ocean acidification [30–32]. By lowering carbonate ion levels and increasing carbonate solubility, ocean acidification is thought to increase the energetic cost of calcification [33] by borrowing energy allocated to other life functions, like reproduction or immunity [34,35]. In contrast, rising water temperature tends to increase growth through increases in metabolism, up to a point where it is no longer energetically favorable to allocate energy towards growth [14,36].

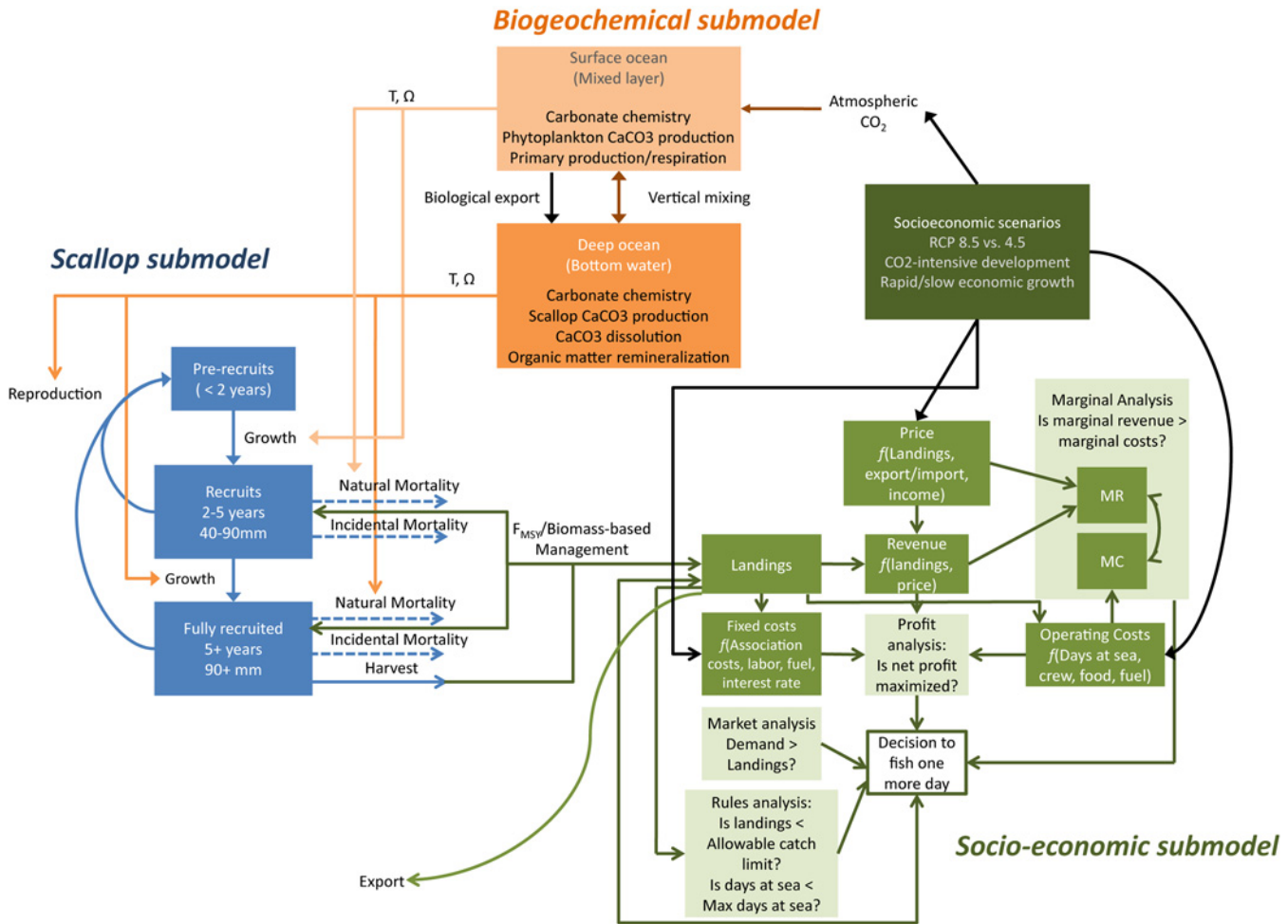## Studies connecting ocean acidification and fisheries harvests

A limited number of studies to date have examined ocean acidification's potential to affect human communities via shellfish harvests. Cooley and Doney [37] reported that ocean acidification-driven losses of ex-vessel revenues could cost the U.S. commercial shellfish fishery a cumulative total of hundreds of millions or billions of US dollars over the next fifty years, depending on discount rate and shellfish responses. There is a similar potential for losses in allied industries. Narita et al. [38] found that global costs of negative ocean acidification-related impacts on commercial shellfish production could exceed $100 billion US annually by 2100, if demand for shellfish rises with future estimated income rise. In addition, ocean acidification could endanger food security for certain seafood-dependent nations [39]. Ocean acidification's impacts on shellfish harvests could be very costly, but detailed policy-relevant information about the relative effects of ocean acidification, rising temperatures, fishing pressure, and socioeconomic factors on specific species has yet to be developed for most species, with a few notable exceptions [10,40]). Recently, Punt et al. [40] linked population and bioeconomic models to project ocean acidification impacts on the Alaskan king crab fishery, providing both management insight and rationale for future studies.

This paper presents a simple IAM that connects reduced-form biogeochemical, population, and economic numerical models for the Atlantic U.S. sea scallop fishery. This model allows investigation of an economically important marine resource in a dynamic system affected by environmental change, fishery policies, and biological stochasticity. A biogeochemical surface-deep box model simulates conditions for sea scallop habitats in Northeast U.S. shelf waters from the present to 2050. Oceanic conditions influence a sea scallop population dynamic model that includes biological stochasticity and realistic harvest pressure. This links to an economic model that projects revenues and costs for the commercial fishery in inflation-adjusted real dollars. This paper describes the model's construction and presents early results based on the business-as-usual RCP 8.5 CO_2 emissions scenario [41] and constant economic growth rates.

Data and Methods

Model design

To build the IAM, three models were developed singly and then linked together (Fig 2). The biogeochemical model is run separately, and then used to force the scallop and socioeconomic models. The biogeochemical submodel (details in Eqs. SI1-10 in S1 Text and Table 1) is a two-box model in which temperature and salinity-driven stratification and mixing govern vertical mixing between the surface and deep (benthic) boxes on the continental shelf [42–44]. The surface—deep two-box model is solved separately for both Georges Bank (GB) and Mid Atlantic Bight (MA) regions at each time step. Carbonate chemistry is fully modeled in each box using the CO2SYS for Matlab software [45,46], including air-sea gas exchange driven by modeled temperatures (Eqs. SI1-SI6 in S1 Text) (Data from NEFSC Oceanography Branch) and wind climatology for 2000–2012 determined from nearby NOAA buoys (NDBC GB Station 44011; MA

Fig 2. Schematic of IAM. Biogeochemical submodel components are orange, scallop submodel components are blue, and socioeconomic submodel components are green.

Station 44009), calcium carbonate production as a function of primary production, a primary production climatology estimated from ocean color data from years 2000–2010, and respiration. The primary productivity climatology utilizes the monthly data (grid size 2160 x 4320) from 2003–2012 [47] (http://www.science.oregonstate.edu/ocean.productivity/index.php). Both wind speeds and primary productivity data vary according to a regular seasonal sinusoid, as expected (Table 1) (for winds, MA: $r^2 = 0.97$, RMSE = 2.85; GB: $r^2 = 0.94$, RMSE = 6.08) (for primary productivity, MA: $r^2 = 0.78$, RMSE = 0.12; GB: $r^2 = 0.96$, RMSE = 0.10). In the biogeochemical model's deep box, calcium carbonate production is explicitly modeled, as is organic matter remineralization. The biogeochemical submodel and the scallop submodel run on the same time step ($\Delta t = 1/10$ yr) which was chosen to be consistent with sea scallop management models currently used by NOAA NMFS [12,17].

The scallop submodel (details in Eqs. SI11-SI18 in S1 Text and Table 2) draws heavily from the von Bertalanffy growth function- (VBGF-) and growth matrix-based [50] population dynamic models used by NOAA for providing management advice to the sea scallop fishery [Scallop Area Management Simulator (SAMS), and the Catch-at-size-analysis (CASA) [12]]. All growth, weight, and mortality parameters were drawn directly from NOAA NMFS

Table 1. Parameters from BGC model.

Parameter	MA	GB	unit	Source	Description
T_1*	13.09	9.51	°C	This study; Data from NEFSC Oceanography	T/S model
T_2*	12.00	10.00	°C		
S_1*	32.22	32.47	psu		
S_2*	32.49	32.44	psu		
$A_{1,T}$	14.48	9.00	N/A		
$A_{1.s}$	-1.46	-0.75	N/A		
$A_{2.T}$	5.21	3.50	N/A		
$\tau_{1,T}$	0.14	0.09	yr^{-1}		
$\tau_{1.S}$	0.11	0.27	yr^{-1}		
τ_2	0.19	0.15	yr^{-1}		
$\varphi_{1,s}$	-0.35	-0.45	yr		
$\varphi_{1.T}$	-0.63	-0.97	yr		
$\varphi_{2.T}$	-1.96	-1.54	yr		
A_{PP}	0.27	0.58	gC m^{-2} d^{-1}	This study; http://www.science.oregonstste.edu/ocean.productivity/index.php	PP
φ_{PP}	-1.92	-2.11	yr		
β_{PP}	1.07	1.04	gC m^{-2} d^{-1}		
Remin	1.00	0.80	N/A	GB [48]; MA:[49]	BGC
PICPOC	0.04	0.04	N/A	Data from NEFSC Oceanography	
F_{ratio}	0.25	0.25	N/A		
K_s	10^{-5}	10^{-5}	m^2 s^{-1}		
h_1	22.00	25.00	m		
h_2	38.00	45.00	m		
A_U	22.74	-33.84	m^2 s^{-1}	This study; Data source NDBC	Wind
φ_U	4.41	4.14	yr		
β_U	52.05	54.23	m^{2}s^{-2}		

Items have different values for Georges Bank (GB) and Mid Atlantic (MA).

doi:10.1371/journal.pone.0124145.t001

documentation [12]. Unlike the SAMS model, the submodel developed here is not completely spatially explicit. It does, however, separate the two populations of Georges Bank (near 41°N, 69°W) and the Mid-Atlantic Bight (near 39°N, 74°W). The model assumes that recruitment is naturally variable each year using random (Gaussian) stochasticity around the stock-recruit relationship.

The socioeconomic submodel (details in Eqs. SI19-SI30 in S1 Text and Table 3) is based on statistical relationships determined through market and economic analyses from NMFS [12,52,53] combined with static economic theory from Moore [54] and economic decision making tools adapted from Nobre et al. [55]. It uses a Cobb-Douglas production function dependent on biomass and number of days fished [56], along with output from the scallop submodel, to estimate industry-wide catches. This production function (Eq. SI19 in S1 Text) was fit to the annual reported landings (NMFS), reported stock biomass [12], and the days at sea (DAS)[52] derived using the vessel trip report (VTR) database [52] from 2000–2009. The production function fit the CASA July 1 biomass and fleetwide DAS very well (Table 2, r^2 = 0.97, p <0.0001), and all coefficients were significant at the 0.99 level. Additionally, autocorrelation and heteroskedasticity were not observed as denoted by a Durbin-Watson test (p = 0.680, DW = 2.61) and a White test (p = 0.343), respectively.

Table 2. Parameters for the scallop submodel.

Parameter	GB	MA	Unit	Source	Description
H_∞	144.9	132.1	mm	[12]	Growth Matrix
σH_∞	14.5	13.1	mm	[12]	
K_i	0.429	0.527	t^{-1}	[12]	
σK_i	0.11	0.135	t^{-1}	[12]	
a_L	23.0	15.5		[12]	Selectivity
b_L	0.221	0.139		[12]	
a_{mw}	-10.70	-10.25		[51]	SH/MW relationship
b_{mw}	2.94	2.85		[51]	
MW_∞	54.7	46.6	g	[12]	
M	0.12	0.15	yr^{-1}	[12]	Natural mortality
I	0.1	0.2	yr^{-1}	[12]	Incidental Mortality
D	0.2	0.2	yr^{-1}	[12]	Discard Mortality
$\ln(a_R)$	20.17	21.35	Millions	[17]	Recruitment
$\sigma ln a_R$	0.202	0.341			
$\ln(\gamma_R)$	6.664	10.073	mT	[17]	
$\sigma ln\gamma_R$	2.871	0.464			
ρ	0.775	0.904			
F_{msy}	0.38	0.38	yr^{-1}	[52]	Fishing mortality
F_{abc}	0.32	0.32	yr^{-1}	[52]	Fishing mortality

Items, except for discard mortality rates, have different values for Georges Bank (GB) and Mid Atlantic (MA).

doi:10.1371/journal.pone.0124145.t002

Table 3. Parameters and quantities in the socioeconomic submodel.

Parameter	Value	Unit	Source	Description
e_p	-0.368	N/A	[54]	Own-price elasticity of demand
e_i	1.83	N/A	[54]	Income elasticity of demand
GRT	166.2	Ton	[12]	Average tonnage
α	1.195	N/A	This study	production function (BIO)
β	0.449	N/A	This study	production function (DAS)
A	-9.95	$lb^{-1} d^{-1}$	This study	production function
Q	Varies	Lb	[12]	Landings
C	S1 Text, Eq. SI27	$	[54]	Total fishery operating costs
w	Varies	$ d^{-1}	[12]	Cost of fishing per day at sea
CREW	7	—	[12]	Average crew per vessel
FUEL	Varies	$ gal^{-1}	[52]	Cost of fuel
DFT	1,0	—	[52]	Indicates dredge or trawl gear
TRW	1,0	—	[52]	Indicates dredge or trawl gear
MC	Eq 1	$ lb^{-1}	This study	Marginal cost
MR	Varies	$ lb^{-1}	This study/[52]	Marginal revenue
MCS	Varies	$ lb^{-1}	This study/[52]	Marginal crew share
$P_{i,t}$	Varies	$ lb^{-1}	[52]	Price of scallops in market class i for year t
MCT_i	Varies	lb^{-1}	[52]	Mean scallop count in market class i
IP_t	Varies	$ lb^{-1}	[52]	Price of imports in year t
R_{fuel}	1.1	%	[12], reference case	Rate of increase of diesel fuel prices

doi:10.1371/journal.pone.0124145.t003

At the beginning of each model year (i.e., the socioeconomic model time step is $10\Delta t$), the socioeconomic model determines industry costs, revenues, and profits by maximizing profits and assuring that hard limits are satisfied (Fig 2). Furthermore, the scallop and socioeconomic models are tightly and explicitly linked through the total catch for the year (Q, lb yr^{-1}), which is determined using data from both the submodels. Scallops caught are removed from each size bin in the scallop submodel to generate landings in the socioeconomic submodel. The number of scallops caught per size class in each time step (Eq. SI16 in S1 Text) is calculated separately for scallop populations in GB and MA, where the total catch (Q_t, Eq. SI17 in S1 Text) determined by the socio-economic submodel is separated into catch from GB and MA by assuming the landings extracted from each location are proportional to the exploitable biomass there (the number of full-grown individuals larger than 90mm). Landings are separated into meat count categories used by the fishery: U10 (10 or fewer scallops lb^{-1}), 11–20 (11–20 scallops lb^{-1}), 21–30 (21–30 scallops lb^{-1}) and 31–40 (31–40 scallops lb^{-1}). Finally, the end of year biomass and the percent of scallops landed by weight in each category are passed from the scallop submodel to the socioeconomic submodel.

Socioeconomic decision making in the model

There are two steps in our model's decision-making process that incorporate elements of the NMFS [12,52,53], Moore [54], and Nobre et al. [55] approaches. The first step is at the management level where rules are developed based on the population model to set the maximum allowable catch. The second step is at the fleet level where maximum allocated days at sea are determined that sustain the maximum allowable catch level, maximize profits, and satisfy an analysis of marginal operating costs, marginal revenues, and national demand.

The management step uses the year-end population distribution to calculate the allowable biological catch (Q_{ABC}) and the maximum allocated days at sea by integrating the scallop submodel (Eq. SI11-SI18 in S1 Text) for a full year and tracking the catch. When determining Q_{ABC}, total fishing mortality is calculated as in Eq. SI14 in S1 Text, but with fishing mortality (F_t) equal to fishing mortality associated with allowable biological catch (F_{ABC}, or 0.32 yr^{-1}), which is a reduction of the current fishing mortality that achieves the maximum sustainable yield (F_{msy}, 0.38 yr^{-1}); this allows for scientific uncertainty. The populations of GB and MA are again tracked separately, and Q_{ABC} is the sum of the catch for the year from each location. This approach for calculating Q_{ABC} is an adaptation of the current area-specific method used in CASA and SAMS.

The second step for the decision-making process first determines the economically optimal catch (Q_t) at the fleet level, which can equal or be lower than the allowable biological catch Q_{ABC}. Current management limits fishing effort by setting the maximum number of days at sea for the entire fleet (DAS_{max}). DAS_{max} is derived from NEFSC relationships that determine landings per unit effort, or number of scallops caught per day at sea. Then Q_{ABC} and DAS_{max} become management-set upper limits for calculating the optimal catch (Q_t) in the socioeconomic submodel.

Next, marginal costs, marginal revenues, and national demand are calculated. Total fishery operating costs (C) are:

$$C = w\left(\frac{Q}{A * BIO^\alpha}\right)^{\frac{1}{\beta}}, \qquad\qquad \text{Eq(1)}$$

assuming static profit maximization as in Moore [54], where w (USD/day) is the cost of fishing per day at sea ([53], presented in Eq. SI27 in S1 Text), and β, α, and A are coefficients from the production function (Table 3). The marginal operating cost (MC) of fishing is the partial

derivative of ([Eq 1](#)) with respect to Q:

$$MC = \frac{\partial C}{\partial Q} = \frac{w}{\beta}\left(\frac{1}{A * BIO^\alpha}\right)^{\frac{1}{\beta}} Q^{\frac{1-\beta}{\beta}} \qquad \text{Eq(2)}$$

where BIO is the total biomass (Eq. SI19 in [S1 Text](#)). More detail is available in [S1 Text](#). In the current industry practice, the operating costs are felt by the crew, rather than the boat owners (e.g. Eqs. SI22-SI26 in [S1 Text](#)), which sets up a socioeconomic tension between scallop crew and scallop boat owners. For example, if the marginal crew income (MCI) is not greater than the marginal cost of fishing, crew would expend more effort for less gain. The MCI is calculated as:

$$MCI = \frac{\partial NCI}{\partial Q} = (\overline{P_{i,t}} - 0.05\overline{P_{i,t}})0.52 - MC, \qquad \text{Eq(3)}$$

where NCI is net crew income, and $\overline{P_{i,t}}$ is the price of scallops (Eq. SI21 in [S1 Text](#)). Future analyses with this model will explore the role of MCI as an additional model diagnostic. As in the Nobre et al. [55] MARKET model, scallop fishermen, including owners and crew, are assumed to be price takers; thus the marginal revenue (MR) is assumed equal to price $\overline{P_{i,t}}$

$$MR = \frac{\partial GR}{\partial Q} = \frac{\partial}{\partial Q} Q_t \overline{P_{i,t}} = \overline{P_{i,t}}. \qquad \text{Eq(4)}$$

Here, GR is gross industry revenue (Eq. SI20 in [S1 Text](#)). To ensure that scallop landings are never in excess of US demand, the US national demand (D_t) for scallops is estimated initially as the sum of landings minus exports plus imports, but afterwards as:

$$D_t = D_{t-1}(1 + r_d). \qquad \text{Eq(5)}$$

where D_{t-1} is the demand from the previous year and r_d is the rate of change of demand between the previous and current years, calculated as in Nobre et al. [55]:

$$r_d = e_p r_p + e_i r_i \qquad \text{Eq(6)}$$

where e_p is the price elasticity of demand [54], r_p is the rate of change in price from the current and previous years, e_i is the income elasticity of demand [54], and r_i is the rate of change in income ([Table 2](#)).

The decision-making component uses Q_{ABC} and DAS_{max} and determines the optimal fleet-wide Q_t and DAS by varying DAS. The decision-making component checks annually to ensure that the following conditions are upheld: profits are maximized, $MC \leq MCI$, $Q_t - export \leq D_t$, $Q_t \leq Q_{ABC}$, and $DAS \leq DAS_{max}$ ([Fig 2](#)). To link the socioeconomic model to the scallop model, the optimal DAS fished are related to fishing mortality F_t (yr^{-1}):

$$F_t = DAS \ F_{das} \qquad \text{Eq(7)}$$

where F_{das} (Eq. SI30 in [S1 Text](#)) is fishing mortality from a single day at sea, DAS is the total number of days fished fleet wide per year. F_t is used as the initial F_t in Equation SI14 in the scallop submodel (see [S1 Text](#)).

Linking the scallop and biogeochemical submodels

There are several ways the biogeochemical model influences the sea scallop model ([Fig 2](#)). The surface box in the biogeochemical model is assumed to influence the larval scallop stage and the deep box is assumed to influence the adult stage. We assume that biogeochemistry can

influence stages of the scallop life cycle by multiple routes: 1) ocean acidification on scallop recruitment, 2) deep water temperature effects on scallop growth, and 3) deep water ocean acidification effects on scallop growth.
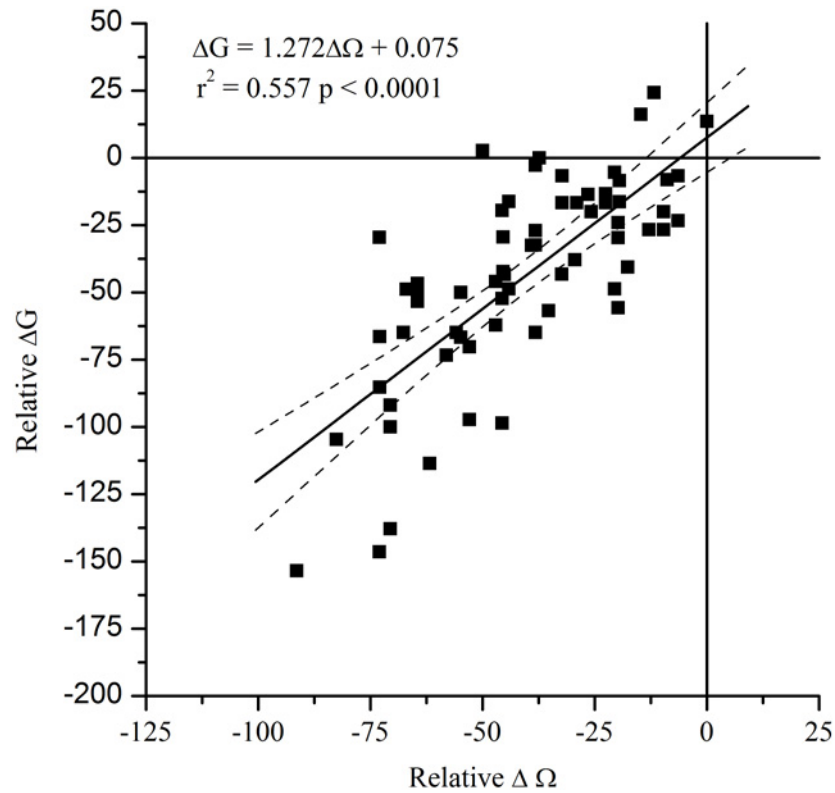
Scallop recruitment may be directly correlated with calcium carbonate saturation state. Recruitment is the number of individuals who survive the larval and juvenile stages to 40mm shell height[57], and this influences the overall stock that survives to grow into harvestable stock. Based on information from other bivalves [26,28,58] including the very similar king scallop (*Pecten maximus L.*) [30], we assume that calcium carbonate saturation state Ω is correlated with sea scallop recruitment. Using the data from Andersen et al. [30] for king scallops, we scale sea scallop larval survival based on the two-year lagged surface Ω_{ar} (saturation state of aragonite) at the time of spawning by:

$$scale\ factor = \frac{\%\ survival}{45\%} = \frac{(20.5\Omega_{ar} - 3.7)}{average\ survival}. \qquad Eq(8)$$

The average larval survival from a given brood is equal to the control survival from the study (45%) [30]. We simulate impacts on recruitment by reducing the spawning stock biomass by the scale factor determined in (Eq 8), which has the effect of reducing larval production by this scale factor. A Beverton-Holt stock-recruit relationship is then used to determine adult recruitment. Although temperature has been hypothesized to affect recruitment in pectinid species [11,59], no quantitative information is available to build a similar scaling relationship for this species, so we did not alter recruitment by temperature in the model.

The model allows deep-water temperature from the biogeochemical model to influence the growth of recruits after settlement in the scallop model. Elevated temperatures increase growth rates and metabolism to a point, then impede growth beyond a limiting high temperature [11,16]. Because scallops recruit at age 2, we used the 2-year lagged mean temperature and allometric relationships described in Heilmayer et al. [36] to calculate the relative change in the Brody growth coefficient (*K*) with temperature and recalculate the growth matrix $\mathbf{G_t}$ for every time step of the scallop model (See Eq. SI12 in S1 Text). This then affects the 'overall growth performance' index (OGP = K^*M_∞), where M_∞ is the mass at size H_∞, the location-specific maximum length (Table 2) [60]. The OGP of different species of scallops can be compared across latitudinal and temperature gradients using an Arrhenius model (See Eqs 2, 5, and Fig 2 in [36]). Temperature does not exceed the maximum value tolerated by this species at any time in the modeled period.

Via a direct correlation, the model also allows decreases in saturation state to decrease both mollusk growth and calcification rate [61,62]. The effects of ocean acidification on *P. magellicanus* have not been studied, so we performed a meta-analysis of literature that reported impacts of ocean acidification on adult mollusk growth or calcification and that was part of the compilation used by Kroeker et al. [62]. We included only bivalves in our analysis, which resulted in 6 studies reporting growth or calcification rates from 8 different species spanning a variety of ecological niches, from intertidal estuarine species to coastal shelf species [27,63–67]. We discarded one study using the Antarctic bivalve *Laternula elliptica* [64] because the slow growth rate of the species resulted in no observed growth from either the control or experimental groups over the timeframe of that study. The resulting data from 7 bivalve species in 5 different studies demonstrated a significant correlation between decreasing saturation state and calcification or growth rate (Fig 3). As these studies were completed using a wide range of saturation states, temperatures, and measured responses, we use the relative change in growth rate or calcification rate from the control compared to the relative change in Ω from the control. For studies that only reported no significant difference, we assume the relative change in growth,

$$\Delta G = 1.272\Delta\Omega + 0.075$$
$$r^2 = 0.557 \; p < 0.0001$$

Fig 3. Relative change in adult/juvenile (>40 mm) bivalve growth or calcification vs. relative change in Ω from literature studies. Includes 8 different species from 6 different studies. Dashed lines are 95% confidence intervals.

doi:10.1371/journal.pone.0124145.g003

ΔG, is 0. The resultant relationship is $\Delta G = 1.272\Delta\Omega + 0.075$ (Fig 3; $r^2 = 0.56$, p <0.0001). To convert between this relationship and the model space, we assume that the Brody growth coefficient K (Eq. SI12 in S1 Text) is directly proportional to the growth or calcification rates reported. Any relative change in growth or calcification rate with saturation state (Fig 3) corresponds to a relative change in K from the control (the initial measured K, Table 1). The change in the growth parameter K due to temperature is calculated (ΔK_T), then the change due to saturation state is calculated separately (ΔK_Ω). To be conservative in our estimates, we assume the changes in growth rate caused by temperature and saturation state occur additively. The value of K, adjusted for temperature and Ω, used in Eq. SI12 in S1 Text then becomes:

$$K_{T,\Omega} = K + \Delta K_T + \Delta K_\Omega. \qquad \text{Eq(9)}$$

Modeled saturation state never drops below the lowest values in observational studies that contributed to this relationship. As saturation state never decreases below $\Omega = 1$ during the period investigated, scallop shells would not be expected to dissolve in situ, and this very minor feedback from scallops to ocean biogeochemistry was not included in the model.

Model initialization and data

The fully coupled IAM was tested by initializing with data from year 2000, and model results were compared to actual landings, revenue, biomass, number, and scallop size distribution from NEFSC for the period 2000–2012 (2009 for biomass and number) and available

Table 4. Initial conditions for the biogeochemical submodel.

Parameter	GB	MA	Unit	Source	Description
T_1	23.29	16.67	°C	NEFSC Oceanography	Surface temperature
T_2	8.52	9.06	°C		Deep temperature
$S1$	31.67	32.19	ppt		Surface salinity
S_2	32.95	32.67	ppt		Deep salinity
DIC_s	1890.1	1987.6	µmol KgSW^{-1}	GOMECCII, R. Wanninkhof, pers. Comm.	Surface DIC
DIC_d	2019.0	2042.8	µmol KgSW^{-1}		Deep DIC
TA_s	2160.6	2206.6	µmol KgSW^{-1}		Surface TA
TA_d	2125.7	2212.4	µmol KgSW^{-1}		Deep TA

Items have different values for Georges Bank (GB) and the Mid Atlantic (MA).

doi:10.1371/journal.pone.0124145.t004

biogeochemical data from the NEFSC Oceanography Branch (temperature and salinity), the gridded SOCAT database (pCO$_2$), and the GOMECC I and GOMECC II cruises (SOCAT:[68], GOMECC I: [24], http://www.aoml.noaa.gov/ocd/gcc/GOMECC1/, GOMECC II: http://www.aoml.noaa.gov/ocd/gcc/GOMECC2/, Wanninkhof pers. comm.). Initial conditions for the BGC model are given in Table 4. The scallop model was initialized with scallop size distribution from the NMFS sea scallop surveys and number of individuals >40mm estimated for July 1, 2000 from the NMFS CASA model. Although the stock-recruit relationships represent the long-term mean in recruitment, there is considerable interannual variability in recruitment in scallop populations. Because interannual variability in recruitment is such a strong driver of sea scallop biomass and abundance, in order to test the model behavior, annual recruitment numbers from the CASA model were used from 2000–2012. The hindcasts also used the reported 2000–2012 per capita disposable income (U.S. Bureau of Economic Analysis, data accessed 10/1/2013), corrected to 2011 dollars using the CPI (Bureau of Labor Statistics, data accessed on 1/16/2014), mean annual import prices (NMFS Foreign Trade, accessed 7/10/2013 corrected to 2011 dollars), and annual scallop exports (NMFS Foreign Trade, accessed 7/10/2013) for the price model. Initial conditions for the scallop and socioeconomic submodels are given in Table 5.

Model sensitivity testing

The model was tested for sensitivity to model parameters by using a Monte Carlo approach [72]. Distributions were assigned to 38 of the model parameters based on either literature values or values were assumed to be multivariate normal from our least squares regressions of the climatologies (Table 1). The model was run for 500 iterations, drawing the parameters from their various distributions. The model was run from 2000–2012 and forced with scallop recruitment values estimated from NMFS survey assessments. Stepwise multiple linear regression was performed by fitting model parameters to the 2012 biomass, landings, and revenues to identify parameters that had the most impact on these model results, which are key indicators describing the social-ecological system (S1 Table).

Results

Scallop model skill

The scallop model (Fig 2, in blue) correctly reproduced the trends in shell height distribution from both locations (Fig 4). During all years, the model scallop size distribution was not significantly different from the whole-stock size distribution reported from the NMFS sea scallop

Table 5. Initial conditions for the socioeconomic and scallop submodels for year 2000.

Parameter	Value	Unit	Source	Description
FC_0	191167	$	[52]	Vessel fixed costs (2001–2007 mean)
$ASSN_0$	1610	$	[52]	Association fees per vessel
$COMM_0$	3446	$	[52]	Communication fees per vessel
BIO_0	172458000	Lb	[12]	Biomass
DAS_0	25849	days	[52]	DAS
$FUEL_0$	1.56	$	[52]	Fuel price
w_0	1184	$/day	[52]	Cost/DAS
$PCDI_0$	25946	$	[69]	Per capita disposable income
D_0	78903000	$	[70,71]	Demand = landings-exports+imports
R_0	3728	millions	D Hart, pers.comm.	CASA recruitment
P_{U10}	8.94	$/lb	[52]	U10 price
P_{1020}	6.73	$/lb	[52]	10–20 price
P_{2030}	6.02	$/lb	[52]	20–30 price
P_{3040}	6.08	$/lb	[52]	30–40 price
LAND	32161800	Lb	[70]	Landings
N_{MA}	3523	millions	[12]	CASA number in MA
N_{GB}	3129	millions	[12]	CASA number in GB
Export	7224800	Lbs	[71]	Exports all scallop
IP0	3.98	$	[71]	Import price
Import	53966000	lbs (all)	[71]	Imports all scallop
$PCTLAND_{U10}$	7	pct	[52]	Percent landed U10
$PCTLAND_{1020}$	20	pct	[52]	Percent landed 11–20
$PCTLAND_{2030}$	42	pct	[52]	Percent landed 21–30
$PCTLAND_{3040}$	21	pct	[52]	Percent landed 31–40

All dollars reported in 2011 USD.

doi:10.1371/journal.pone.0124145.t005

surveys using 2-sample Kolmogorov-Smirnov tests (MA: $p > 0.05$, KSstat < 0.369; GB: $p > 0.05$, KSstat < 0.312, n = 22 for all years).

Whole stock modeled biomass (Fig 5A) and abundance (Fig 5B) agreed with CASA modeled whole stock July 1 biomass and abundance from 2000–2009 [12]. Mean CASA July 1 scallop abundance was 6654 million individuals (range 5933–7446) and scallop biomass was 113790 metric tons (mT) meats (range 78390–129703). Mean modeled abundance was 7528 million individuals (range 6652–8724) and biomass was 118200 mT meats (range 78390–131450). The average absolute model-data error for abundance and biomass was 15.3 ± 12.6% and 3.97 ± 5.03% (SD, n = 10), respectively.

Scallop landings by size class determined from the population model also agreed well with trends in landings from 2000–2012 (Fig 6) and accounted for changes in gear selectivity, which occurred several times throughout the period, that select for larger sized scallops. Mean reported and modeled U10 scallop landings from this time period were 12.9% (range 3–24%) and 7.9% (range 1.2–11.6%), respectively. Mean 11–20 reported and modeled landings were 47.6% (range 14–77%) and 74.4% (range 20.0–85.7%), respectively. Mean 21–30 reported and modeled landings were 29.0% (range 6–66%) and 13.8% (range 5.2–42.0%), respectively. Mean 31–40 reported and modeled landings were 3.7% (range 0–21%) and 3.2% (range 0.5–21%), respectively [52]).

Fig 4. A) Actual and (B) modeled relative scallop shell height distribution from Georges Bank based on number of individuals in each 5mm size class. Data from D. Hart, from NMFS scallop surveys. Data from year 2000 are model initial conditions.

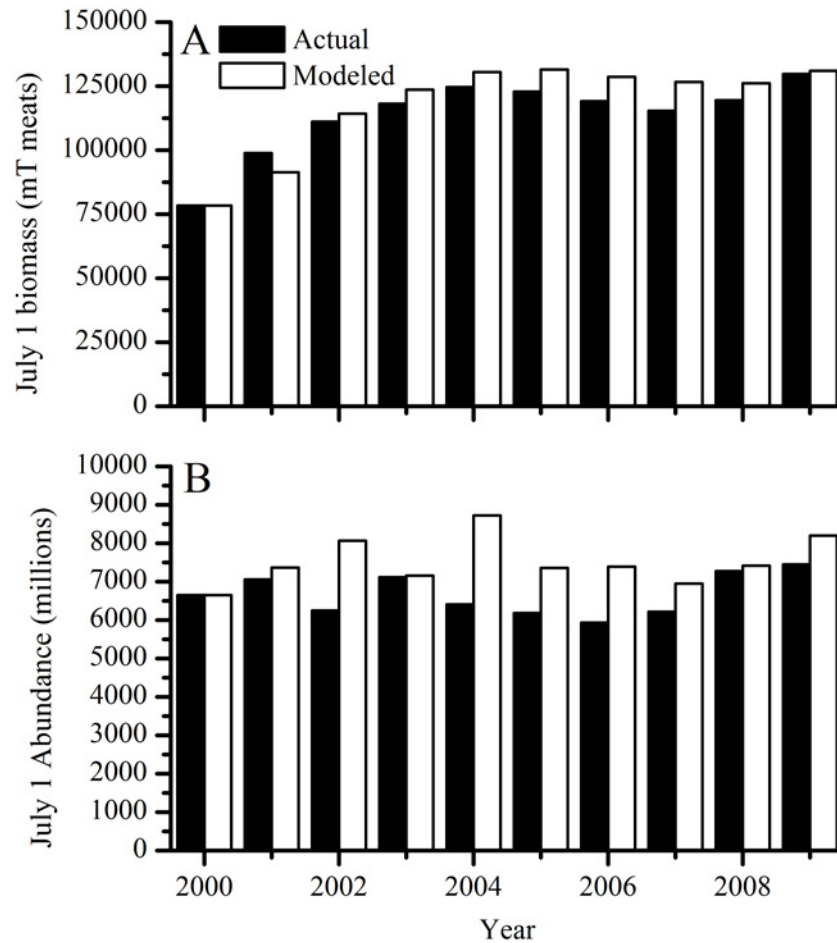doi:10.1371/journal.pone.0124145.g004

Economic model skill

Scallop ex-vessel prices matched well the reported prices in both trend and magnitude (not shown) resulting in revenues that agree well with the reported revenues (Fig 7A) and landings (Fig 7B) from 2000–2012. Mean annual reported and modeled revenue for this period was 349 million USD (range 157–573 million USD) and 343 million USD (range 149–483 million USD), respectively. Mean annual reported and modeled landings were 24835 mT meats (range 14619–29140 mT meats) and 20535 mT meats (range 12713–25528 mT meats), respectively. Average absolute model-data error in revenues and landings was 13.2 ± 11.5% and 19.1 ± 17.2%, respectively (SD, n = 13).

Biogeochemical model skill

The simplified two box model reproduced seasonal cycles of temperature, salinity, and annual water column stratification and mixing well (Fig 8). Model RMSE for the surface and deep temperature was 1.58 and 1.31°C, respectively and RMSE for the surface and deep salinity was 0.39 and 0.37 psu, respectively.

Fig 5. Actual (NEFSC 2010, CASA estimated July 1) and modeled whole stock (A) biomass and (B) abundance. Data from year 2000 are model initial conditions.

The magnitude and timing of seasonal cycles of DIC and TA agree well with model estimates from the global Community Earth System Model (not shown), producing pCO_2 values that agree very well between the two models in both the surface and deep boxes (Fig 9), as well as with the gridded SOCAT surface pCO_2 data available from the representative model region (Fig 9A)[73] and the profiles from the GOMECC I and II cruises (Fig 10). Modeled pCO_2 values are consistently somewhat (~30 ppm) lower than the ranges reported by Rebuck and Hare [23]. Normalized RMSE of the model and SOCAT pCO_2 database for GB was 7.0% and for MA was 13.2%. Model-data residuals from both GB and MA do not have observable patterns across the time series and are normally distributed (KS test, $p = 0.459$, KS stat = 0.133, $n = 39$ for GB; $p = 0.759$, KS stat = 0.114, $n = 32$ for MA).

Model sensitivity

Of the 500 Monte Carlo simulations, 67 did not converge because the gear selectivity fished out the largest scallops quickly. The remaining 433 simulations showed wide variability in 2012 biomass (S2 Fig), landings and revenue, ranging from 30400–265000 mT, 1910–42500 mT, and 4.0–79 million 2011 USD, respectively. Stepwise MLR identified 10 total parameters that

Fig 6. (A) Actual data from NMFS (may not add up to 100%) and (B) modeled scallop landings by category. Category represents range of meat count/lb. Actual data reported in [52](may not add up to 100). Note actual 2012 from months 1–3. Data from year 2000 are model initial conditions.

doi:10.1371/journal.pone.0124145.g006

were significantly driving the model results explaining 79.3, 86.3, and 78.9% of the variability in biomass, landings, and revenue, respectively (S2 Table).

Fully integrated scenarios

Model runs varied beyond 2012 owing to stochastic recruitment (Fig 10). Under the RCP8.5 scenarios until 2050, projected mean annual surface box pH decreases from 8.05 to 7.91 in MA and from 8.08 to 7.94 in GB, respectively. Projected deep box pH decreases from 8.05 to 7.85 in MA and from 8.05 to 7.89 in GB, respectively. Projected Ω (calcite) in the surface box decreases from 3.35 to 2.65 in MA and from 3.23 to 2.51 in GB, respectively. Projected Ω (calcite) in the deep box decreases from 2.64 to 1.99 in MA and from 2.80 to 2.11 in GB, respectively (shown for GB in Fig 10A and 10B). Under the constant CO_2 scenario, projected total landings (Fig 10C), biomass (Fig 10D), revenues (Fig 10E), and distribution of landings by size class (e.g. Fig 10F,

Fig 7. Actual (NMFS commercial landings accessed Jan. 28, 2014) and modeled ex-vessel (A) revenue and (B) landings. Data from year 2000 are model initial conditions.

shown for U10) stabilize after 2020, but decrease under the RCP8.5 scenario. Compared to the constant CO_2 scenario, under the climate change scenario RCP8.5, the percent of landings from the largest category of scallops (U10) decreased from a mean ± SD of 11.0 ± 0.3% in 2012 to 6.6 ± 0.5% in 2050 (Fig 10A).
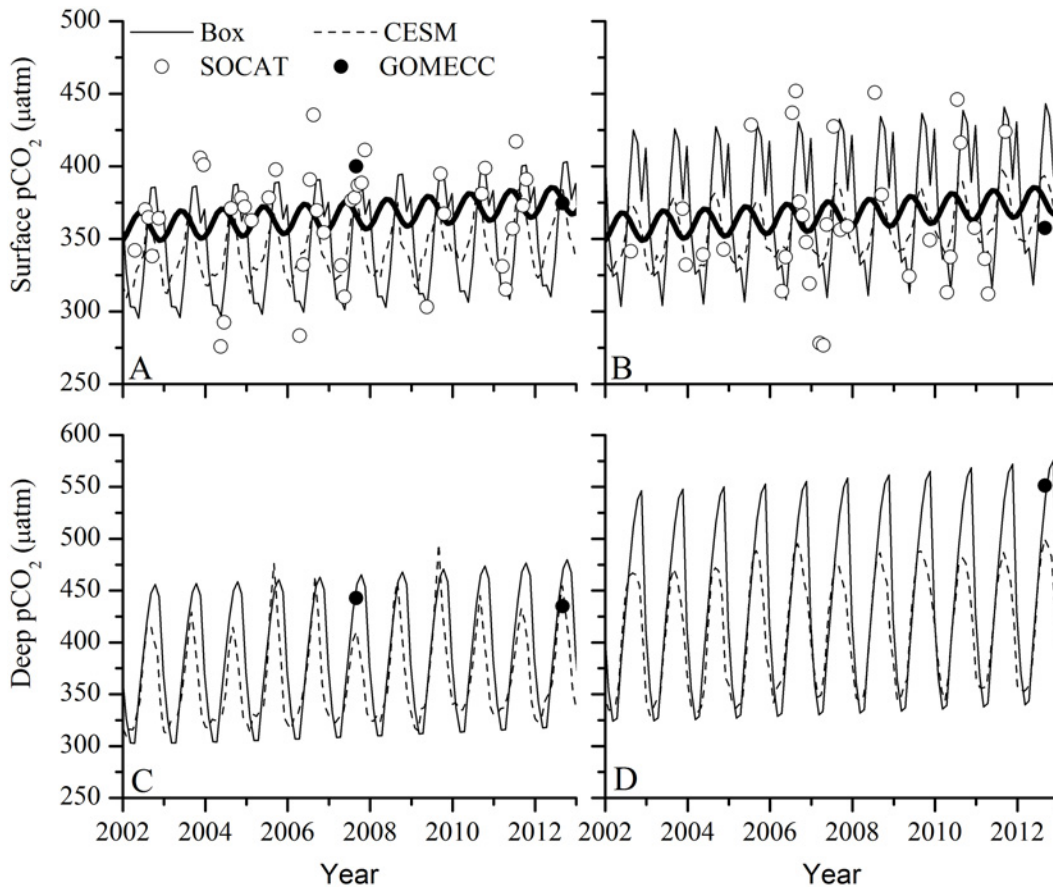
Discussion

The development of this sea scallop IAM offers new possibilities for considering anthropogenically driven global change in fisheries harvest planning. Because our primary goal is to enrich resource management deliberations by offering both short- and long-term insight into the system rather than to replace current fisheries management models, our simplified, modular approach to building this IAM is appropriate. It can be easily updated as new information becomes available, and complexity can be built into the submodels as research questions demand.

When run under "control" conditions, or present-day CO_2 and harvest levels held constant through time, the model demonstrates stable behavior and good skill in reproducing the past ten years of harvests. Model deviations from the observed parameters are explained either by spatially explicit details we did not include in the model (e.g., rotational management and closed areas) or by natural processes (e.g. a massive die-off of large scallops between 2004 and 2004 in MA populations [75]) that occurred during some years. For example, the model's underestimation of the relative number of scallops in the largest size class in both MA and GB (Fig 4) is because rotational management practices and permanently closed areas that NMFS uses to maximize scallop biomass and yield are not included in the model. This management scheme allows scallops to grow very large in areas closed to fishing and thus attain sizes that

Fig 8. Salinity, salinity residuals, temperature, and temperature residuals from the two box models (solid) calibrated to data collected during bimonthly oceanographic cruises (dashed) within a 1° x 1° area representative of conditions on (A—D) Georges Bank and (E—H) in the Mid-Atlantic. Surface conditions are given in red and bottom conditions are given in blue. Data from NEFSC Oceanography branch.
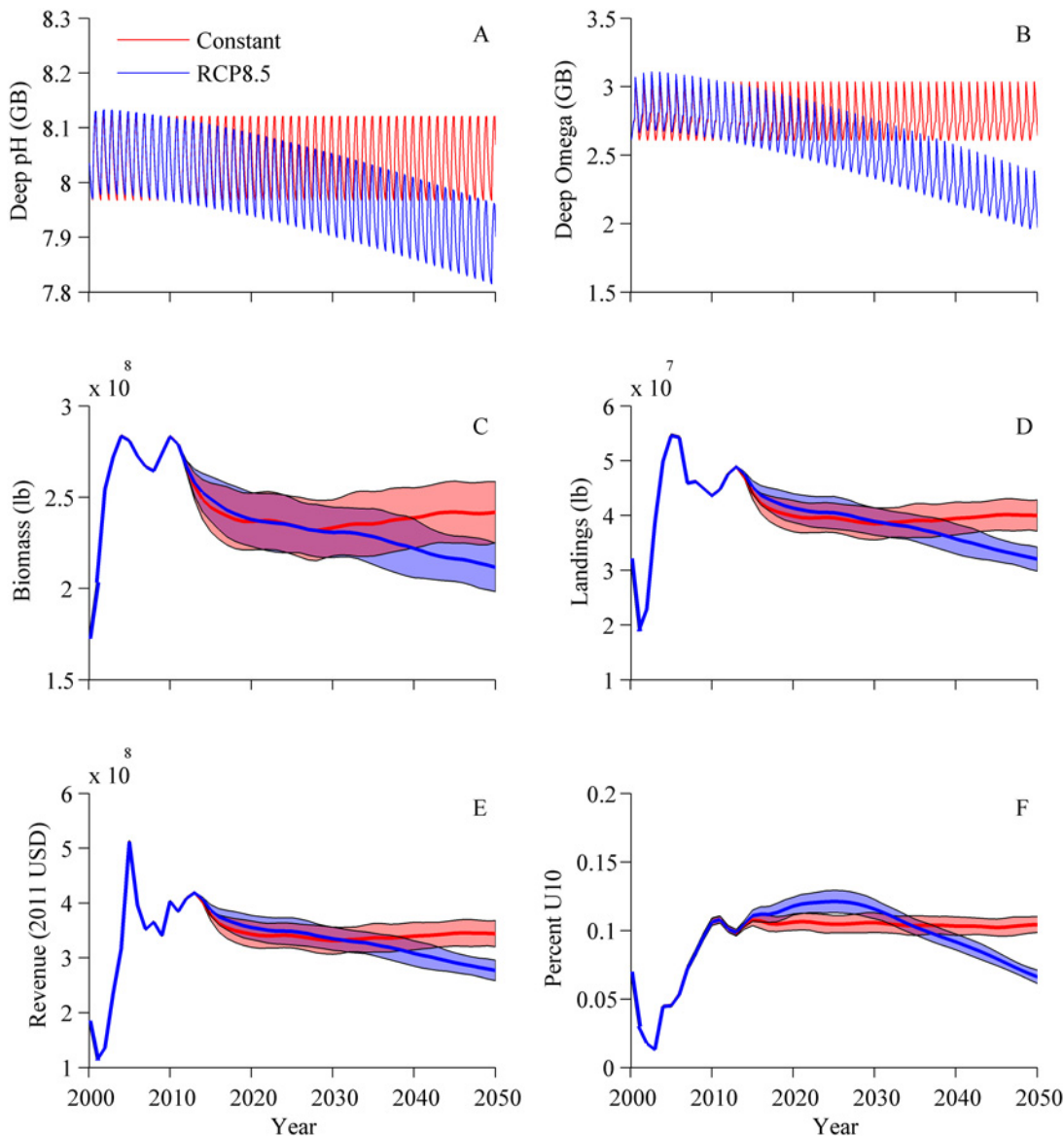
Fig 9. (A) Georges Bank and (B) Mid-Atlantic surface pCO_2 from the box model (solid), the global CESM model (dashed), and atmospheric CO_2 forcing (heavy solid). Open circles are from the SOCAT gridded database [68] and closed circles are from the GOMECC I [24] and II (Wanninkhof pers. comm) cruises in 2007 and 2012. (C) Georges Bank and (D) Mid-Atlantic deep pCO_2 from the box model (solid) and the global CESM model (dashed)[74].

doi:10.1371/journal.pone.0124145.g009

are at or larger than the modeled H_∞, while in the model, scallops are removed as they enter the larger size bins. The model overestimates biomass and abundance in 2004 compared to observations (Fig 5) because a large die-off of small scallops between 2003 and 2004 occurred in MA populations [75], which was not incorporated into the model. This causes the model to overestimate abundance for several years afterwards as the extra scallops grow and are harvested. Finally, the large difference in landings and revenues in the early 2000s (Fig 7) is due to changes in selectivity imposed in the model to reflect NMFS altered selectivity periods (2001–2003, 2004–2012 in GB, see NEFSC 2010 Figure B-26). During the 2001–2003 period, NMFS uses a domed selectivity for GB to simulate a large biomass of scallops that were located in closed areas, and thus unavailable for harvest [12,17]. Using domed selectivity is one method for including spatial variability such as marine protected areas into fisheries population models [76] but it does not provide the best possible model-data fit for this species [17]. We expect that these deviations would decrease if our model included more spatially explicit details.

The simple biogeochemical model containing the major oceanographic features relevant in the GB and MA regions, temperature and salinity-driven mixing and air-sea CO_2 uptake, reproduced observations of carbonate chemistry well in these regions. The good agreement between modeled and surface pCO_2 from the SOCAT database (NRMSE 13.2% for MA and 7.6% for GB) from both regions suggests that the model parameterizations are capturing the major

Fig 10. Mean ± SD (n = 100) model forecasts out to 2050 using CO$_2$ forcing from RCP 8.5 and 1.4°C SST warming (blue) and forecasts with constant 2008 CO$_2$ concentration and temperature (red). Deep box (A) pH and (B) calcite saturation state from Georges Bank, (C) landings, (D) total spawning stock biomass (scallops >40mm shell height), (E) revenue (2011 USD), and (F) fractional landings in category U10 (meat weight 10 and under scallops/lb).

processes that drive the local carbonate chemistry. Furthermore, the modeled deep carbonate chemistry agreed well with data from the two GOMECC cruises, although more observations would be necessary to evaluate this component of the model in detail. The more complex oceanographic features of each region, such as horizontal flow, were omitted for simplicity, and leaving them out did not noticeably decrease the skill of the biogeochemical submodel.

A central challenge of building this model is that no studies of ocean acidification's effects have been completed on *P. magellanicus*. To close this data gap, we parameterized growth rate and saturation state for post-settlement adults using a relationship based on other adult bivalve responses, but this has limitations. Despite the availability of studies correlating saturation state and physiological processes, no mechanistic relationship has been proposed to date that

links these variables; saturation state is only a proxy for what is likely to be several linked causal mechanisms. The studies used to develop this statistical relationship span a wide range of pH values which are more extreme than those likely to influence scallops by 2100, raising the question of whether this relationship is driven by these extremes. For example, the control values ranged from 8.15–7.99, while the experimental values ranged from 8.09–7.00, depending on source water and pCO_2 experimental treatment. Restricting our analysis to only values that might be expected by 2100 (pH declines of <0.3), this relationship is still significant and fairly strong for saturation state (p <0.0001, $n = 49$, $F_n = 54.45$, $r^2 = 0.29$). If we include studies on bivalves identified as juveniles into the analysis, this adds an additional 8 studies and 5 species [32,58,77–82] bringing the total to 13 separate studies with 12 different species. Although this would increase the scatter in our relationship, a significant decline in relative growth still occurs with saturation state (see S2 Fig), further supporting our approach. Although we are confident that this relationship is appropriate for the purposes of this study, intraspecific variability in adult responses has been noted [83]. Another unanswered question is whether the timing of early larval CO_2 exposure that affects later development in other species [84,85] might also occur in *P. magellanicus*.

Ideally, directly measured relationships between growth rate, survival, saturation state and temperature would exist for larvae, juveniles, and adults. But these studies have not been completed for *P. magellanicus* at this time. Our assumption that the relationships between life processes and saturation state or temperature are additive is a simplification. Synergistic effects of multiple stressors like acidification and temperature have been observed (e.g., [86–89]) and changes in organism performance noted at higher temperatures [34] can alter organisms' energy budgets and govern their responses to environmental change. Although our modeled temperatures do not exceed the maximum thermal tolerance of *P. magellanicus*, it is likely that at the southern limit, or in inshore habitats, temperatures may exceed this threshold under future warming scenarios. If this is the case, our assumption that temperature will only increase growth may be overestimating scallop production in future projections. However, we believe our approach is appropriate given the very limited experimental data available for this species, and that spatially explicit physical modeling of the US East Coast shelf is beyond the scope of this model.

Another assumption in our model is the treatment of scallop recruitment. Because of the lack of species-specific information on pre-recruits [40,90], we chose to impact scallop recruitment only through the stock-recruit relationship rather than developing a specific pre-recruit model as Punt et al. did for king crab [40]. A reduction in scallop recruitment due to ocean acidification could be a result of many processes that occur between spawning and scallop recruitment, such as decreases in gamete production, fertilization, larval survival, or growth and mortality of juveniles. Depending on the shape of the stock-recruit relationship, this may not affect the fishery in intuitive ways. In Georges Bank, the stock-recruit relationship is flat, and reductions in larval survival would only slightly influence recruitment because it is not thought to be limited by larval supply [12,16]. This may be partly due to the nature of local currents which retain larvae within the gyre over Georges Bank [91]. Rather, recruitment may be limited by other factors such as predation, food availability or suitable habitat for settlement. In areas where the stock-recruit relationship is more linear, this is an indication that recruitment may be limited by larval supply [12,16], and reductions in larval survival will influence recruitment substantially. For example, using specified model parameters for both GB and MA for the stock recruit relationships and modeled stock, if larval survival is reduced by 50%, in the Mid-Atlantic, recruitment would be reduced by 24%, while on Georges Bank, recruitment would only be reduced by 1.6%. The major assumptions required to build this model highlight the strong need for studies of the effects of ocean acidification and warming on *P. magellanicus*

given its large economic importance and relatively unique life history characteristics (e.g., oceanic, mobile adults) compared to other bivalve species harvested by commercial fisheries in the U.S.

The model indicates that with business-as-usual CO_2 emissions (RCP 8.5), the assumed additive effects of warming and acidification, and the present harvest rules, sea scallop populations and harvests could decline over time. By 2050, average landings of large scallops and total overall landings could decrease ([Fig 10]). The antagonistic interaction of warming increasing growth rates, ocean acidification slowing growth rates, and interannual variability in recruitment masks any negative influence of ocean acidification in the short term. Interestingly, increased growth rates from warming outweigh decreasing growth rates from ocean acidification until 2030 when the negative influence of ocean acidification overtakes warming; this can be seen in the larger contribution of U10 scallops to the total landings from approximately 2015–2035 compared to the constant CO_2 scenario ([Fig 10F]). Beyond 2030, in an ocean undergoing acidification plus further warming, whose net effect shifts to slow overall growth rates, fewer scallops attain U10 size before they are harvested if current fishing levels are maintained. This is because present scallop harvest minimum sizes and allowable catch limits are optimized for a population that is not experiencing progressive externally imposed environmental pressure. As ocean acidification advances, growth slows even farther, and present-day harvest rules (with fixed F_{msy}, F_{ABC} and fishery selectivity) become increasingly out of step with the resulting population distribution. This highlights the need to understand ocean acidification's effect on *P. magellanicus* and the importance of managing fishery populations in full acknowledgment of the reality that management will occur against a backdrop of progressive change, rather than constancy. As U10 size scallops bring a higher price than other sizes, this result is quite interesting from an economic perspective, and bears further investigation in future analyses using this model.

Conclusions

The IAM developed in this study represents another step towards regular inclusion of anthropogenically driven global change into fisheries harvest planning. This IAM for the U.S. *P. magellanicus* fishery rigorously incorporates the known, published mechanisms that govern scallop growth, relationships between scallops and their environment, and market dynamics. It is a tool that can be used to explore different combinations of catch limits, temperature, acidification, and even different scallop life-history responses to acidification. Model sensitivity testing indicates that the key life history and fishery parameters (natural and incidental mortality, shell height-meat weight relationships, and selectivity) will be critical to understanding the impacts of ocean acidification on the social-ecological system. Importantly, the model can also be revised as knowledge develops concerning the response of sea scallops to ocean acidification, because several possible impact pathways (on scallop recruitment, growth, and mortality) are explicitly parameterized. Initial runs of the model, assuming continued present-day fishery mortality rates, business-as-usual CO_2 emissions, a linear negative relationship between ocean acidification and sea scallop growth, and additive interactions of warming and ocean acidification indicate an overall decline in scallop harvests, an initial increase followed by a decline in U10 (largest market size class) scallops, and an accompanying decrease in revenue. Future work will explore different economic and management scenarios and test how potential impacts of ocean acidification on other scallop biological parameters may influence the social-ecological system. In this way, the model complements the population dynamic models used now for fisheries management by providing a window into the broader social-ecological system and the long-term context in which the sea scallop fishery operates. This information will

allow managers to make informed decisions that plan for both short- and long-term processes that affect the U.S. sea scallop fishery, a perspective that will also be useful in other high-value, single species fisheries elsewhere.

Supporting Information

S1 Fig. Relative change in adult (>40 mm) and juvenile bivalve growth or calcification vs. relative change in (A) pH or (B) Ω from literature studies. Includes 14 different species from 10 different studies. Blue lines are trends using adult only (Fig 3) and red lines are trends using both adult and juvenile studies. Dashed lines are 95% confidence intervals.
(TIF)

S2 Fig. Biomass from Monte Carlo model runs. Thick line is the mean value over 433 model runs, shaded area is ± SD, dashed lines are maximum and minimum values for the model runs.
(TIF)

S1 Table. Model sensitivity analysis parameters and distributions.
(DOCX)

S2 Table. Stepwise multiple linear regression of model parameters to 2012 biomass and landings.
(DOCX)

S1 Text. Equations for the oceanographic, population dynamic, and socioeconomic submodels.
(DOCX)

Acknowledgments

Author Contributions

Conceived and designed the experiments: SRC SCD JAH DRH DMG. Performed the experiments: SRC JER VL. Analyzed the data: SRC JER VL. Contributed reagents/materials/analysis tools: DRH SCD DMG. Wrote the paper: SRC JER DRH DMG JAH SCD.

References

1. Pauly D, Christensen V, Dalsgaard J, Froese R, Torres F. Fishing down marine food webs. Science. 1998; 279: 860–863. doi: 10.1126/science.279.5352.860 PMID: 9452385

2. Cheung WWL, Watson R, Pauly D. Signature of ocean warming in global fisheries catch. Nature. 2013;497. doi: 10.1038/nature12156 PMID: 24048473

3. Cheung WWL, Dunne J, Sarmiento JL, Pauly D. Integrating ecophysiology and plankton dynamics into projected maximum fisheries catch potential under climate change in the Northeast Atlantic. Ices J Mar Sci. 2011; 68: 1008–1018. doi: 10.1093/icesjms/fsr012

4. Sumaila UR, Cheung WWL, Lam VWY, Pauly D, Herrick S. Climate change impacts on the biophysics and economics of world fisheries. Nat Clim Change. 2011; 1: 449–456. doi: 10.1038/nclimate1301

5. Stramma L, Prince ED, Schmidtko S, Luo J, Hoolihan JP, Visbeck M, et al. Expansion of oxygen mini-mum zones may reduce available habitat for tropical pelagic fishes. Nat Clim Change. 2012; 2: 33–37. doi: 10.1038/NCLIMATE1304

6. Hare JA, Alexander MA, Fogarty MJ, Williams EH, Scott JD. Forecasting the dynamics of a coastal fish-ery species using a coupled climate-population model. Ecol Appl. 2010; 20: 452–464. doi: 10.1890/08-1863.1 PMID: 20405799

7. Doney SC. The growing human footprint on coastal and open-ocean biogeochemistry. Science. 2010; 328: 1512–1516. doi: 10.1126/science.1185198 PMID: 20558706

8. Fulton EA, Smith ADM, Smith DC, van Putten IE. Human behaviour: the key source of uncertainty in fisheries management. Fish Fish. 2011; 12: 2–17. doi: 10.1111/j.1467-2979.2010.00371.x

9. Hollowed AB, Barange M, Beamish RJ, Brander K, Cochrane K, Drinkwater K, et al. Projected impacts of climate change on marine fish and fisheries. ICES J Mar Sci J Cons. 2013; 70: 1023–1037. doi: 10.1093/icesjms/fst081

10. Kaplan IC, Levin PS, Burden M, Fulton EA. Fishing catch shares in the face of global change: a frame-work for integrating cumulative impacts and single species management. Can J Fish Aquat Sci. 2010; 67: 1968–1982. doi: 10.1139/F10-118

11. Hart DR, Chute AS. Essential fish habitat source document: Sea scallop, *Placopecten magellanicus*, life history and habitat characteristics, 2nd edition. [Internet]. U.S. Department of Commerce, National Marine Fisheries Service, Northeast Fisheries Science Center; 2004 Sep p. 32. Report No.: NMFS-NE-189. Available: http://www.nefsc.noaa.gov/nefsc/publications/tm/tm189/tm189.pdf

12. Northeast Fisheries Science Center. 50th Northeast Regional Stock Assessment Workshop (50th SAW): 50th SAW Assessment Report. 2010.

13. MacDonald BA, Thompson RJ. Influence of temperature and food availability on the ecological energet-ics of the giant scallop *Placopecten magellanicus*. II. Reproductive output and total production. Mar Ecol Prog Ser. 1985; 25: 295–303.

14. Hart DR, Chute AS. Estimating von Bertalanffy growth parameters from growth increment data using a linear mixed-effects model, with an application to the sea scallop *Placopecten magellanicus*. Ices J Mar Sci. 2009; 66: 2165–2175. doi: 10.1093/icesjms/fsp188

15. National Marine Fisheries Service. Fisheries of the United States 2012 [Internet]. Fisheries Statistics Di-vision, National Oceanic and Atmospheric Administration; 2012 Aug. Report No.: 2012. Available: http://www.st.nmfs.noaa.gov/commercial-fisheries/fus/fus12/index

16. Hart DR, Rago PJ. Long-term dynamics of US Atlantic sea scallop *Placopecten magellanicus* popula-tions. North Am J Fish Manag. 2006; 26: 490–501. doi: 10.1577/M04-116.1

17. Hart DR, Jacobson LD, Tang J. To split or not to split: Assessment of Georges Bank sea scallops in the presence of marine protected areas. Fish Res. 2013; 144: 74–83. doi: 10.1016/j.fishres.2012.11.004

18. Hare JA, Manderson JP, Nye JA, Alexander MA, Auster PJ, Borggaard DL, et al. Cusk (*Brosme brosme*) and climate change: assessing the threat to a candidate marine fish species under the US En-dangered Species Act. ICES J Mar Sci J Cons. 2012; 69: 1753–1768. doi: 10.1093/icesjms/fss160

19. Doney SC, Balch WM, Fabry VJ, Feely RA. Ocean acidification: A critical emerging problem for the ocean sciences. Oceanography. 2009; 22: 36–47.

20. Wanninkhof R, Park G-H, Takahashi T, Sweeney C, Feely R, Nojiri Y, et al. Global ocean carbon up-take: magnitude, variability and trends. Biogeosciences. 2013; 10: 1983–2000. doi: 10.5194/bg-10-1983-2013

21. Feely RA, Doney SC, Cooley SR. Ocean acidification: present conditions and future changes in a high-CO2 world. Oceanography. 2009; 22: 36–47.

22. Bindoff NL, Willebrand J, Artale V, Cazenave A, Gregory J, Gulev S, et al. Observations: oceanic cli-mate change and sea level. Climate Change 2007: The Physical Science Basis Contribution of Working Group I to the Fourth Assessment Report of the Intergovernmental Panel on Climate Change. United Kingdom and New York, NY, USA: Cambridge University Press; 2007.

23. Rebuck N, Hare JA. Historical and regional variability in the carbonate system of the US Northeast Shelf. Cont Shelf Res. in prep.; PMID: 21984862

24. Wang ZA, Wanninkhof R, Cai W-J, Byrne RH, Hu X, Peng T-H, et al. The marine inorganic carbon sys-tem along the Gulf of Mexico and Atlantic coasts of the United States: Insights from a transregional coastal carbon study. Limnol Oceanogr. 2013; 58: 325–342. doi: 10.4319/lo.2013.58.1.0325

25. Miller AW, Reynolds AC, Sobrino C, Riedel GF. Shellfish face uncertain future in high CO$_2$ world: influ-ence of acidification on oyster larvae calcification and growth in estuaries. Finkel Z, editor. PLoS ONE. 2009; 4: e5661. doi: 10.1371/journal.pone.0005661 PMID: 19478855

26. Talmage SC, Gobler CJ. Effects of past, present, and future ocean carbon dioxide concentrations on the growth and survival of larval shellfish. Proc Natl Acad Sci. 2010; doi: 10.1073/pnas.0913804107

27. Gazeau F, Quiblier C, Jansen JM, Gattuso J-P, Middelburg JJ, Heip CHR. Impact of elevated CO_2 on shellfish calcification. Geophys Res Lett. 2007;34. doi: 10.1029/2006GL028554

28. Talmage SC, Gobler CJ. The effects of elevated carbon dioxide concentrations on the metamorphosis, size, and survival of larval hard clams (*Mercenaria mercenaria*), bay scallops (*Argopecten irradians*), and Eastern oysters (*Crassostrea virginica*). Limnol Oceanogr. 2009; 54: 2072–2080.

29. Green MA, Waldbusser GG, Reilly SL, Emerson K, O'Donnell S. Death by dissolution: Sediment saturation state as a mortality factor for juvenile bivalves. Limnol Oceanogr. 2009; 54: 1037–1047.

30. Andersen S, Grefsrud ES, Harboe T. Effect of increased pCO(2) level on early shell development in great scallop (*Pecten maximus Lamarck*) larvae. Biogeosciences. 2013; 10: 6161–6184. doi: 10.5194/bg-10-6161-2013

31. Schalkhausser B, Bock C, Stemmer K, Brey T, Pörtner H-O, Lannig G. Impact of ocean acidification on escape performance of the king scallop, *Pecten maximus*, from Norway. Mar Biol. 2013; 160: 1995–2006. doi: 10.1007/s00227-012-2057-8

32. Sanders MB, Bean TP, Hutchinson TH, Le Quesne WJF. Juvenile king scallop, *Pecten maximus*, is potentially tolerant to low levels of ocean acidification when food is unrestricted. PloS One. 2013;8. doi: 10.1371/journal.pone.0074118

33. Fabry VJ, Seibel BA, Feely RA, Orr JC. Impacts of ocean acidification on marine fauna and ecosystem processes. ICES J Mar Sci. 2008; 65: 414–432. doi: 10.1093/icesjms/fsn048

34. Poertner H-O. Ecosystem effects of ocean acidification in times of ocean warming: a physiologist's view. Mar Ecol-Prog Ser. 2008; 373: 203–217. doi: 10.3354/meps07768

35. Wood HL, Spicer JI, Widdicombe S. Ocean acidification may increase calcification rates, but at a cost. Proc R Soc B-Biol Sci. 2008; 275: 1767–1773. doi: 10.1098/rspb.2008.0343 PMID: 18460426

36. Heilmayer O, Brey T, Pörtner HO. Growth efficiency and temperature in scallops: a comparative analysis of species adapted to different temperatures. Funct Ecol. 2004; 18: 641–647. doi: 10.1111/j.0269-8463.2004.00905.x

37. Cooley SR, Doney SC. Anticipating ocean acidification's economic consequences for commercial fisheries. Environ Res Lett. 2009; 4: 024007. doi: 10.1088/1748-9326/4/2/024007

38. Narita D, Rehdanz K, Tol RSJ. Economic costs of ocean acidification: a look into the impacts on global shellfish production. Clim Change. 2012; doi: 10.1007/s10584-011-0383-3 PMID: 24014154

39. Cooley SR, Lucey N, Kite-Powell HL, Doney SC. Nutrition and income from mollusks today imply vulnerability to ocean acidification tomorrow. FISH Fish. 2012; 13: 182–215. doi: 10.1111/j.1467-2979.2011.00424.x PMID: 23268745

40. Punt AE, Poljak D, Dalton MG, Foy RJ. Evaluating the impact of ocean acidification on fishery yields and profits: The example of red king crab in Bristol Bay. Ecol Model. 2014; 285: 39–53. doi: 10.1016/j.ecolmodel.2014.04.017

41. Van Vuuren DP, Edmonds J, Kainuma M, Riahi K, Thomson A, Hibbard K, et al. The representative concentration pathways: an overview. Clim Change. 2011; 109: 5–31. doi: 10.1007/s10584-011-0148-z

42. Archer D. Upper ocean physics as relevant to ecosystem dynamics: A tutorial. Ecol Appl. 1995; 5: 724–739. doi: 10.2307/1941980

43. Kuhlbrodt T. T, Titz S, Feudel U, Rahmstorf S. A simple model of seasonal open ocean convection Part II: Labrador Sea stability and stochastic forcing. Ocean Dyn. 2001; 52: 0036–0049. doi: 10.1007/s10236-001-8175-3

44. Rahmstorf S. A simple model of seasonal open ocean convection Part I: Theory. Ocean Dyn. 2001; 52: 0026–0035. doi: 10.1007/s10236-001-8174-4

45. Dickson AG, Sabine CL, Christian JR, editors. Guide to Best Practices for Ocean CO_2 Measurements [Internet]. 2007. Available: http://cdiac.ornl.gov/oceans/Handbook_2007.html

46. Van Heuven S, Pierrot D, Rae JWB, Lewis E, Wallace DWR. MATLAB Program Developed for CO_2 System Calculations. ORNL/CDIAC-105b. [Internet]. Oak Ridge, Tennessee: Carbon Dioxide Information Analysis Center, U.S. Department of Energy; 2011. Available: 10.3334/CDIAC/otg. CO2SYS_MATLAB_v1.1

47. Behrenfeld MJ, Falkowski PG. Photosynthetic rates derived from satellite-based chlorophyll concentration. Limnol Oceanogr. 1997; 42: 1–20. doi: 10.4319/lo.1997.42.1.0001 PMID: 11541205

48. MacKinnon JA, Gregg MC. Mixing on the late-summer New England shelf—solibores, shear, and stratification. J Phys Oceanogr. 2003; 33: 1476–1492. doi: 10.1175/1520-0485(2003)033<1476:MOTLNE>2.0.CO;2

49. Kemp PF, Falkowski PG, Flagg CN, Phoel WC, Smith SL, Wallace DWR, et al. Modeling vertical oxygen and carbon flux during stratified spring and summer conditions on the continental shelf, Middle

Atlantic Bight, eastern U.S.A. Deep Sea Res Part II Top Stud Oceanogr. 1994; 41: 629–655. doi: 10.1016/0967-0645(94)90038-8

50. Caswell H. Matrix population models: construction, analysis, and interpretation. Sunderland, Mass.: Sinauer Associates; 2001.

51. Hennen DR, Hart DR. Shell height-to-weight relationships for Atlantic sea scallops (*Placopecten magellanicus*) in offshore U.S. waters. J Shellfish Res. 2012; 31: 1133–1144. doi: 10.2983/035.031.0424

52. New England Fishery Management Council. Framework 24 to the Scallop FMP and Framework 29 to the Multispecies FMP. 2012.

53. New England Fishery Management Council. Final Framework 22 to the Scallop FMP. 2011.

54. Moore CC. Welfare impacts of ocean acidification: An integrated assessment model of the US mollusk fishery. National Center for Environmental Economics: U.S. Environmental Protection Agency; 2011 Dec. Report No.: 11–06.

55. Nobre AM, Musango JK, de Wit MP, Ferreira JG. A dynamic ecological-economic modeling approach for aquaculture management. Ecol Econ. 2009; 68: 3007–3017. doi: 10.1016/j.ecolecon.2009.06.019

56. Edwards SF. Rent-seeking and property rights formation in the U.S. Atlantic sea scallop fishery. Mar Resour Econ. 2001; 16. Available: http://ideas.repec.org/a/ags/mareec/28123.html

57. Hart DR. Yield- and biomass-per-recruit analysis for rotational fisheries, with an application to the Atlantic sea scallop (*Placopecten magellanicus*). Fish Bull. 2003; 101: 44–57.

58. Talmage SC, Gobler CJ. Effects of elevated temperature and carbon dioxide on the growth and survival of larvae and juveniles of three species of northwest Atlantic bivalves. Plos One. 2011; 6. doi: 10.1371/journal.pone.0026941

59. Shephard S, Beukers-Stewart B, Hiddink JG, Brand AR, Kaiser MJ. Strengthening recruitment of exploited scallops Pecten maximus with ocean warming. Mar Biol. 2010; 157: 91–97. doi: 10.1007/s00227-009-1298-7

60. Brey T. Population dynamics in benthic invertebrates. A virtual handbook. Version 01.2 [Internet]. 2001. Available: http://www.thomas-brey.de/science/virtualhandbook

61. Kroeker KJ, Micheli F, Gambi MC, Martz TR. Divergent ecosystem responses within a benthic marine community to ocean acidification. Proc Natl Acad Sci U S A. 2011; 108: 14515–14520. doi: 10.1073/pnas.1107789108 PMID: 21844331

62. Kroeker KJ, Kordas RL, Crim R, Hendriks IE, Ramajo L, Singh GS, et al. Impacts of ocean acidification on marine organisms: quantifying sensitivities and interaction with warming. Glob Change Biol. 2013; 19: 1884–1896. doi: 10.1111/gcb.12179 PMID: 23505245

63. Mingliang Z, Jianguang F, Jihong Z, Bin L, Shengmin R, Yuze M, et al. Effect of marine acidification on calcification and respiration of *Chlamys farreri*. J Shellfish Res. 2011; 30: 267–271. doi: 10.2983/035.030.0211

64. Cummings V, Hewitt J, Van Rooyen A, Currie K, Beard S, Thrush S, et al. Ocean acidification at high latitudes: potential effects on functioning of the Antarctic bivalve *Laternula elliptica*. PLoS ONE. 2011; 6: e16069. doi: 10.1371/journal.pone.0016069 PMID: 21245932

65. Ries JB, Cohen AL, McCorkle DC. Marine calcifiers exhibit mixed responses to CO_2-induced ocean acidification. Geology. 2009; 37: 1131–1134. doi: 10.1130/G30210A.1

66. Thomsen J, Melzner F. Moderate seawater acidification does not elicit long-term metabolic depression in the blue mussel *Mytilus edulis*. Mar Biol. 2010; 157: 2667–2676. doi: 10.1007/s00227-010-1527-0

67. Melzner F, Stange P, Trübenbach K, Thomsen J, Casties I, Panknin U, et al. Food supply and seawater pCO_2 impact calcification and internal shell dissolution in the blue mussel *Mytilus edulis*. PLoS ONE. 2011; 6: e24223. doi: 10.1371/journal.pone.0024223 PMID: 21949698

68. Bakker DCE, Pfeil B, Smith K, Hankin S, Olsen A, Alin SR, et al. An update to the Surface Ocean CO_2 Atlas (SOCAT version 2). Earth Syst Sci Data. 2014; 6: 69–90. doi: 10.5194/essd-6-69-2014

69. U.S. Bureau of Economic Analysis. Table 2.1. Personal Income and its Disposition [Internet]. Available: http://www.bea.gov/iTable/iTable.cfm?ReqID=9&step=1#reqid=9&step=3&isuri=1&910=x&911=0&903=58&904=2000&905=2013&906=a

70. U.S. National Marine Fisheries Service. Commercial Landings [Internet]. 2013. Available: http://www.st.nmfs.noaa.gov/commercial-fisheries/commercial-landings/annual-landings/indexdata

71. U.S. National Marine Fisheries Service. Foreign Trade [Internet]. 2013. Available: http://www.st.nmfs.noaa.gov/commercial-fisheries/foreign-trade/applications/annual-product-by-countryassociation

72. Schouten M, Verwaart T, Heijman W. Comparing two sensitivity analysis approaches for two scenarios with a spatially explicit rural agent-based model. Environ Model Softw. 2014; 54: 196–210. doi: 10.1016/j.envsoft.2014.01.003

73. Signorini SR, Mannino A, Najjar RG, Friedrichs MAM, Cai W-J, Salisbury J, et al. Surface ocean pCO_2 seasonality and sea-air CO_2 flux estimates for the North American east coast. J Geophys Res Oceans. 2013; 118: 5439–5460. doi: 10.1002/jgrc.20369

74. Long MC, Lindsay K, Peacock S, Moore JK, Doney SC. Twentieth-century oceanic carbon uptake and storage in CESM1(BGC)*. J Clim. 2013; 26: 6775–6800. doi: 10.1175/JCLI-D-12-00184.1

75. Stokesbury KDE, Carey JD, Harris BP, OKeefe CE. Incidental fishing mortality may be responsible for the death of ten billion juvenile sea scallops in the mid-Atlantic. Mar Ecol Prog Ser. 2011; 425: 167–173. doi: 10.3354/meps09020

76. Sampson DB, Scott RD. A spatial model for fishery age-selection at the population level. Can J Fish Aquat Sci. 2011; 68: 1077–1086. doi: 10.1139/f2011-044

77. Parker LM, Ross PM, O'Connor WA. Populations of the Sydney rock oyster, *Saccostrea glomerata*, vary in response to ocean acidification. Mar Biol. 2011; 158: 689–697. doi: 10.1007/s00227-010-1592-4

78. Range P, Chícharo MA, Ben-Hamadou R, Piló D, Matias D, Joaquim S, et al. Calcification, growth and mortality of juvenile clams *Ruditapes decussatus* under increased pCO_2 and reduced pH: Variable responses to ocean acidification at local scales? J Exp Mar Biol Ecol. 2011; 396: 177–184. doi: 10.1016/j.jembe.2010.10.020

79. Michaelidis B, Ouzounis C, Paleras A, Portner H-O. Effects of long-term moderate hypercapnia on acid-base balance and growth rate in marine mussels *Mytilus galloprovincialis*. Mar Ecol Prog Ser. 2005; 293: 109–118.

80. Berge JA, Bjerkeng B, Pettersen O, Schaanning MT, Øxnevad S. Effects of increased sea water concentrations of CO_2 on growth of the bivalve *Mytilus edulis L*. Chemosphere. 2006; 62: 681–687. doi: 10.1016/j.chemosphere.2005.04.111 PMID: 15990149

81. Fernndez-Reiriz MJ, Range P, lvarez-Salgado XA, Labarta U. Physiological energetics of juvenile clams *Ruditapes decussatus* in a high CO_2 coastal ocean. Mar Ecol Prog Ser. 2011; 433: 97–105. doi: 10.3354/meps09062

82. Duarte C, Navarro JM, Acuña K, Torres R, Manríquez PH, Lardies MA, et al. Combined effects of temperature and ocean acidification on the juvenile individuals of the mussel *Mytilus chilensis*. J Sea Res. 2014; 85: 308–314. doi: 10.1016/j.seares.2013.06.002

83. Gazeau F, Parker LM, Comeau S, Gattuso J-P, O'Connor WA, Martin S, et al. Impacts of ocean acidification on marine shelled molluscs. Mar Biol. 2013; 160: 2207–2245. doi: 10.1007/s00227-013-2219-3

84. White MM, McCorkle DC, Mullineaux LS, Cohen AL. Early exposure of bay scallops (*Argopecten irradians*) to high CO_2 causes a decrease in larval shell growth. PLoS ONE. 2013; 8: e61065. doi: 10.1371/journal.pone.0061065 PMID: 23596514

85. White MM, Mullineaux LS, McCorkle DC, Cohen AL. Elevated pCO_2 exposure during fertilization of the bay scallop Argopecten irradians reduces larval survival but not subsequent shell size. Mar Ecol Prog Ser. 2014; 498: 173–186. doi: 10.3354/meps10621

86. Calosi P, Donohue P, Alber S, Spicer JI. Synergistic effect of ocean acidification and elevated temperature on the physiological ecology of the intertidal crab *Porcellana platycheles*. Comp Biochem Physiol-Mol Integr Physiol. 2009; 153A: S169. doi: 10.1016/j.cbpa.2009.04.351

87. Gobler CJ, DePasquale EL, Griffith AW, Baumann H. Hypoxia and acidification have additive and synergistic negative effects on the growth, survival, and metamorphosis of early life stage bivalves. PLoS ONE. 2014; 9: e83648. doi: 10.1371/journal.pone.0083648 PMID: 24416169

88. Rosa R, Seibel BA. Synergistic effects of climate-related variables suggest future physiological impairment in a top oceanic predator. Proc Natl Acad Sci U S A. 2008; 105: 20776–20780. doi: 10.1073/pnas.0806886105 PMID: 19075232

89. Russell BD, Thompson J-AI, Falkenberg LJ, Connell SD. Synergistic effects of climate change and local stressors: CO_2 and nutrient-driven change in subtidal rocky habitats. Glob Change Biol. 2009; 15: 2153–2162. doi: 10.1111/j.1365-2486.2009.01886.x

90. Richards RG, Davidson AT, Meynecke J-O, Beattie K, Hernaman V, Lynam T, et al. Effects and mitigations of ocean acidification on wild and aquaculture scallop and prawn fisheries in Queensland, Australia. Fish Res. 2015; 161: 42–56. doi: 10.1016/j.fishres.2014.06.013

91. Gilbert CS, Gentleman WC, Johnson CL, DiBacco C, Pringle JM, Chen C. Modelling dispersal of sea scallop (*Placopecten magellanicus*) larvae on Georges Bank: The influence of depth-distribution, planktonic duration and spawning seasonality. Prog Oceanogr. 2010; 87: 37–48. doi: 10.1016/j.pocean.2010.09.021